2014 IEEE International Conference on Robotics & Automation (ICRA)
Hong Kong Convention and Exhibition Center
May 31 - June 7, 2014. Hong Kong, China

Energy Efficient UAS Flight Planning for Characterizing Features of Supercell Thunderstorms

Jack Elston[1] and Brian Argrow[2]

Abstract— **This work considers a new application area for autonomous soaring through the examination of the energetic environment contained in supercell thunderstorms in an effort to extend sampling mission duration. It identifies the gust front associated with the rear-flank downdraft of the supercell thunderstorm as an interesting candidate for such a mission, and examines the potential for soaring in the region. This knowledge is combined with sampling techniques employed in previous field experiments to produce an energy efficient path at an altitude and location identified as an interesting area for in situ sampling. The path is tested using a flight through simulated storm data, and is shown to provide a net positive gain in energy to the vehicle. This encouraging result indicates the possibility of extending the sampling mission from its current limited length to a significant portion of the storm evolution, a capability that could provide invaluable information about the causes of tornadogenesis.**

I. INTRODUCTION

The primary objective of the second Verification of the Origins of Rotation in Tornadoes Experiment (VORTEX2) was to increase understanding of tornadogenesis - the process of tornado formation [1]. A consensus of research in the last 25 years makes it clear that a small downdraft of a few kilometers width, known as the rear-flank downdraft (RFD) plays a causative role in tornado formation [2]. Unfortunately, access to the RFD for remote and in situ measurements is difficult using contemporary measurement techniques. While weather radar can return detailed precipitation and wind-field data, it cannot return directly-measured thermodynamic data. Balloons cannot be constrained to a sampling region after release, and provide only serial ascents. Furthermore, although flows around the RFD have been sampled by manned aircraft [3], manned assets for storm sensing are hard to obtain, are relatively expensive, and risk human life.

During VORTEX2 a small unmanned aircraft system (sUAS) was used to sample this this difficult region of the storm. Despite successfully intercepting six supercell thunderstorms, two of which were tornadic, several areas for improvement of the sUAS were identified. Among these was increasing the endurance of the observations. Generally, the sUAS was able to fly missions lasting thirty minutes to an hour depending on the wind environment [4]. Some of this time was used for ingress and egress, and limited sampling time such that only a few transects of the area of interest could be performed. Although this still provided information critical to understanding the thermodynamic properties of the storm, the sampling window was too short to provide a good understanding of the storm evolution.

Autonomous soaring has been shown in both simulation and flight tests to increase the endurance of sUAS. Recent work has focused on the development of automatic control algorithms for harvesting energy from relatively static features such as thermals [5] or ridge lift [6]. These algorithms exploit the structure of updrafts to keep the aircraft within an area where it can gain energy, leaving the updraft to perform any secondary tasks, or when the updraft's potential has dissipated. Other efforts have focused on utilizing wind-field gradients to add energy to the aircraft [7], [8], [9]. That work generally considers short flight paths designed to benefit from structure of the wind field, and links the flight paths in a manner which achieves a set of sensing goals. Limited work has also focused on energy extraction from gusts [10]. This requires a reactive technique to make use of the short term effects of turbulence to impart small amounts of energy to the vehicle.

Effective use of static and dynamic soaring require knowledge about the local wind environment. Given that sUAS are typically operated in clear air environments where measurements of the global wind field are not available, the information must be gathered during the mission or provided *a priori* to the controller. *A priori* knowledge of the wind field given is usually limited to the region around geographic features such as mountain ridges, ocean waves, and other surface features as they produce known gradient fields that can generate sufficient lift or shear to sustain flight. This paper presents a proposal to exploit the unique environment of supercell thunderstorms, where fine-scale dual-Doppler RADAR measurements are commonly available (even if not in real-time), and the structure of the storm is relatively well known on a large scale [3]. A synthesis of these two information sources provides significant knowledge of the wind environment, and can be leveraged for path planning. An example of this has been demonstrated through simulation to provide feasible paths through the storm environment [11].

II. ENERGY HARVESTING

Static soaring makes use of vertical winds to impart energy to an aircraft. These winds can be generated in a variety of ways, but are typically due to convection or the interaction of surface winds with terrain. The convection-generated lift occurs over regions where the surface is warmer than the surrounding area. This produces a column of rising air,

[1]Jack Elston is a Posdoctoral Researcher in the Department of Aerospace Engineering Sciences, University of Colorado Boulder, Boulder, CO 80309, USA jack.elston@colorado.edu

[2]Brian Argrow with the Department of Aerospace Engineering Sciences, Univeristy of Colorado Boulder, Boulder, CO 80309, USA brian.argrow@colorado.edu

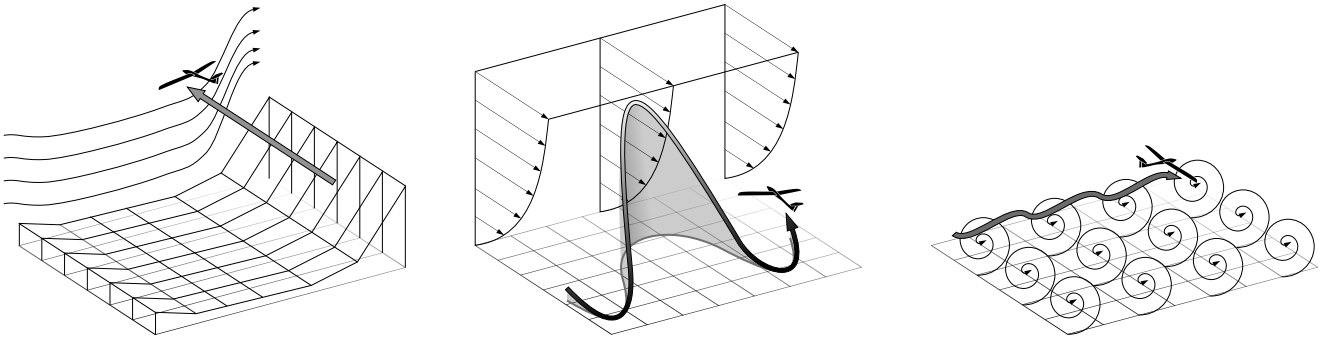

Fig. 1. a) Static soaring, b) dynamic soaring, c) gust energy extraction

known as a thermal, which can impart sufficient energy to sustain gliding flight by manned aircraft. Terrain features can also create regions of rising air, particularly around ridges and mountains. Orographic lift, or ridge lift, is caused when horizontal winds are pushed over a rise in the terrain. Larger features, such as mountains, can also produce lift downstream of their interaction with the wind in the form of lee waves which can reach heights several times that of the obstacle.

Dynamic soaring exploits gradients in a wind field to impart energy to an airborne body. As this process was first described in relation to the energy efficient flights of birds over the ocean [12], a significant body of work has been performed to describe flight over large bodies of water. This includes the fundamental work performed by Lissaman [8]and Sachs [7] to use dynamic equations to describe the energy extraction methods, and comment on the minimum shear required to sustain flight. It has been further extended through the work of Richardson [9] who parameterized the various aspects of the required flight path, and considered additional energy extraction through boundary layer processes in the presence of ocean waves. Other studies have also examined ridge soaring [13], [14], [15], utilizing natural gradients from a terrestrial boundary layer [16], and even generic wind structures [17].

Figure 1 graphically depicts dynamic and static soaring, as well as energy extraction from gusts. Although energy from gusts might be viable for a sUAS, particularly in the turbulent storm environment, the remainder of this work will focus on static and dynamic soaring. Considering the state of the art for both radar systems and storm simulations, fine scale turbulence will be difficult to resolve, effectively providing an unknown environment similar to studies that have already been conducted [10]. Furthermore, given supercell thunderstorms are defined by large regions of strong convection, energy extraction using static soaring is a much more likely candidate for certain locations within the storm. Dynamic soaring is similarly attractive given the large gradients present in the boundaries between the various inflows and outflows.

To examine the utility of static soring in the supercell environment, the work of Depenbusch [18] is used to define the change in total energy state for gliding through a given region of the storm. Given an aircraft with wing area S flying at airspeed v_a in the presence of inertial wind components w_x and w_z, the change in total energy can be defined as:

$$\dot{e}_{tot} = -w_z + \frac{qS}{mg}(-C_D + C_T \cos\alpha)v_a - \frac{\dot{w}_x}{g}\cos\gamma + \frac{\dot{w}_z}{g}v_a \sin\gamma \tag{1}$$

given dynamic pressure is defined as $q = \frac{1}{2}\rho v_a^2$, C_D and C_T represent the coefficient of drag and the coefficient of thrust, α is the angle of attack, and γ is the vertical rotation between the wind axis and inertial axis. To simplify this examination, α is assumed to be constant and equal to the angle of attack at the cruise speed of the aircraft. The coefficient of drag is approximated using the equation

$$C_D = C_{D_0} + C_{D_\alpha}\alpha \tag{2}$$

where C_{D_0} is the parasitic drag coefficient,and C_{D_α} is the induced drag coefficient.

Evaluation of dynamic soaring for use in energy harvesting requires a different approach. While it is possible for energy gain from static soaring to be realized at each instance during a flight, the nature of dynamic soaring requires that a flight path is defined and the energy evaluated over the path length to determine a net energy gain. This energy gain is evaluated using equations presented by Gao [16]. The rate of change of energy in a dynamic soaring application is defined as:

$$\dot{e}_{tot} = -\frac{dw_x}{dz}v_a^2 \sin\gamma\cos\gamma\sin\psi - \frac{Dv_a}{m} \tag{3}$$

the aerodynamic drag, D, is determined using the following equation

$$D = \frac{1}{2}\rho S C_D v_a^2 \tag{4}$$

and the coefficient of drag, C_D, is determined by the equation

$$C_D = C_{D_0} + \frac{C_L^2}{\pi e AR} \tag{5}$$

where C_L is the coefficient of lift, AR is the aspect ratio, and e is Oswalds's efficiency factor.

III. Simulated Storm Examination

Previous work resulted in a simulation capability developed to combine storm data from simulated and measured sources with a high-fidelity unmanned aircraft (UA) dynamic

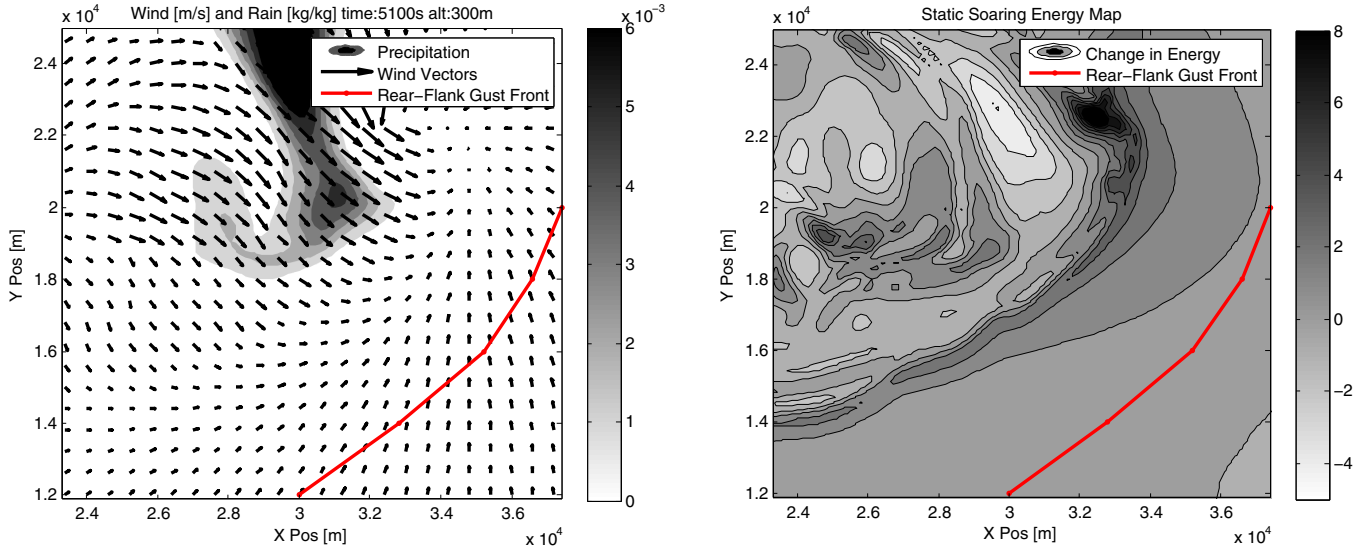

Fig. 2. a) Precipitation and horizontal winds for same section of the thunderstorm for identifying structure of the storm. b) Energy map for static soaring generated from simulated supercell thunderstorm data.

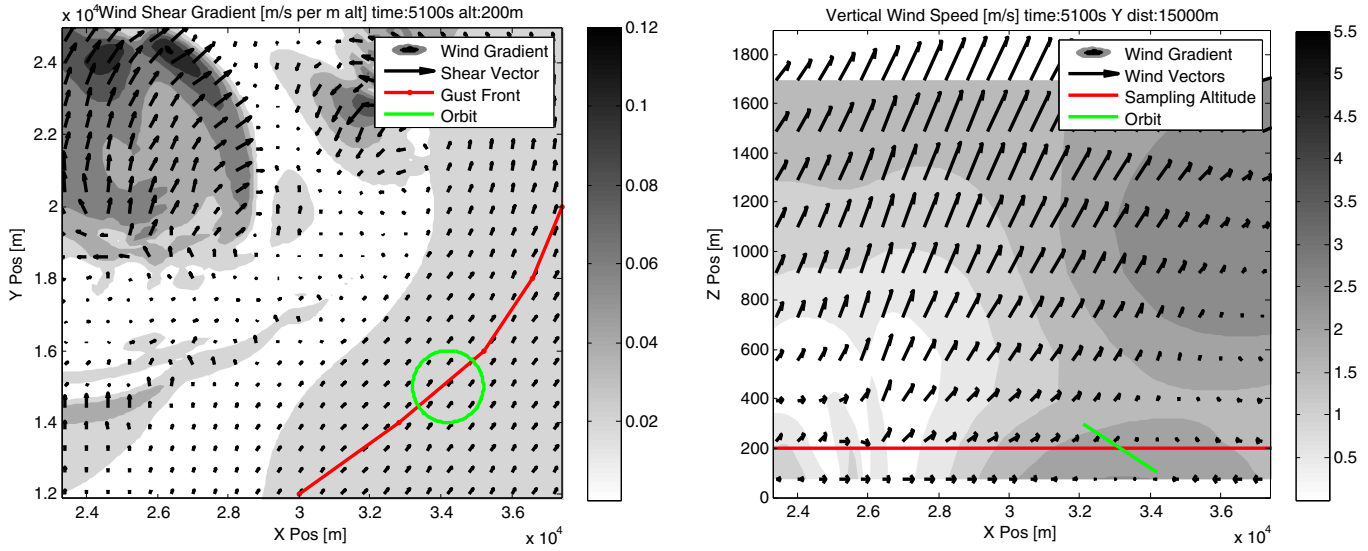

Fig. 3. a) Storm data in the 200 meter plane, with the shading indicating the wind gradient. b) Storm data at in the plane $y = 15000$, with the shading indicating the wind gradient.

model [19]. The simulation has been designed to utilize data sets generated from simulations of tornadic supercell thunderstorms produced by the Straka Atmospheric Model[20]. The storm parameters for the data set used here are given on a 480×480×10 grid with 150 m horizontal spacing and a stretched vertical grid spacing containing 10 altitudes from 750 m to 1694 m above ground level (AGL). Simulated measurements include rain, hail, and three-dimensional wind velocity components relative to the storm frame of reference, provided every five minutes for 20 minutes. The storm simulation is aligned such that the positive y-axis corresponds to north, and the storm is moving at 19 m/s to the east and 2 m/s to the north. Rain contours and wind components for this data set are shown in Figure 2(a).

Equation 1 is applied to the simulated supercell data to identify potential regions for static soaring. The aircraft parameters for Equation 1 are derived from the Tempest sUAS used in the VORTEX2 field campaign (Table I or [21]), or are approximated from similar aircraft. The results can be seen in Figure 2(b). To create this energy map, the UA is assumed to be performing horizontal transects of the storm at 300 m, and γ is set to zero. Also, w_x is assumed to be the magnitude of the wind interpolated from the wind velocities provided at each grid location. This accounts for the worst case scenario where the UA is flying directly into the wind. A quick glance at the energy map reveals that even with these

TABLE I
TEMPEST UAS PARAMETERS

Characteristic	Value	Units
Wingspan	3.22	m
Wing Area	0.63	m^2
Mass	6.4	kg
Aspect Radio	16.2	
C_{D_0}	0.03	
C_{D_α}	0.3	
e	0.9	
Glide ratio	40	

pessimistic assumptions, several areas of the storm support a positive change in energy and therefore possess the potential for sustained flight.

Upon closer examination, however, the regions with the strongest updrafts are not in ideal locations for a sampling mission. As can be seen at the top of the rear-flank gust front (RFGF) in Figure 2(a), the reason for the strong updraft in the region is its proximity to the location of the tornado, indicated by the convergence of the cyclonic winds in this region. The other potential location for static soaring, located at the coordinates $(2.45\times10^4, 1.95\times10^4)$, appears promising, but upon examination of a time series of the data, turns out to be a very short-lived feature. Therefore, although the available data limits the examination to a 20 minute segment of the storm's evolution, static soaring appears to be a poor choice for energy harvesting.

As an alternative, dynamic soaring is considered. Although complete circuits are required to provide an analysis of the energy that can be extracted using this method at a given point on the map, Lissaman's work indicates that a minimum linear shear gradient, S, for energy-neutral cycles is given by $S = 4.75/G$ where G is the maximum L/D [8]. In the case of the Tempest this is approximately 0.12. Figure 3(a) shows the shear gradient at the chosen sampling altitude of 200 m. Unfortunately, similar to static soaring the areas that would best support soaring are either located too close to the location of the tornado, or are in short lived features. However, a region of shear does exist around the RFGF, and while not large enough in magnitude to sustain energy neutral flight, will add to the total sUAS energy making use of dynamic soaring.

IV. SIMULATION

To continue the examination of the potential for dynamic soaring techniques to extend mission duration, several flights were conducted through the simulated storm data. The concept of operations was based on a derivation of the UAS scientific objectives defined by the VORTEX2 project. This assumes the RFD of a supercell thunderstorm as the feature of interest, and identifies sampling patterns, sampling altitudes and desired sampling times. The 2010 field component of the VORTEX2 work identified and utilized three sampling techniques designed to fit the requirements of the regulatory and vehicle constraints imposed on the project [4]. For one of these techniques, the UA flies east-west transects out to 5 km either side of the RFGF up to 300 m AGL, starting from a launch point ahead of the storm (Figure 4). This provides the best opportunity for performing multiple transects before the storm moves out of range.

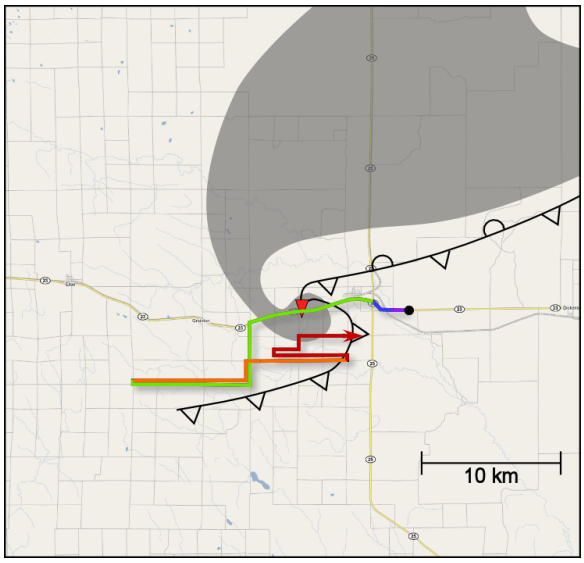

Fig. 4. Deployment scenario from the VORTEX2 campaign, the gray outline represents the shape of the component of the storm visible on RADAR, and the colored track indicates the intended path and altitude of the aircraft.

Combining the scientific goals with the analysis from the previous section, a sampling pattern was chosen that consists of an orbit centered on the RFGF, approximately 5 km south of the hook echo (Figure 3(a)). The altitude of the orbit descends linearly from west to east to produce a pattern able to take advantage of the environment's wind gradient in combination with the updraft present behind the gust front (Figure 3(b)). This altitude change is set at 100 meters on either side of the intended 200 meter sampling altitude. While this height change is larger than typical dynamic soaring altitude deviation, it allows for the vehicle to both remain closer to the ground at the lowest part of the orbit, while pushing higher toward the stronger updrafts on the opposing side. For control of the aircraft the desired height, h_D, is defined by the equation:

$$h_{\mathrm{D}} = -\cos(\psi_{\mathrm{O}}) \times h_\delta + h_{\mathrm{S}} \tag{6}$$

where h_S is the sampling altitude, h_δ is the max deviation from the sampling altitude, and ψ_{O} is the angle from the UA to the center of its orbit, defined by

$$\psi_{\mathrm{O}} = \tan^{-1}\left(\frac{y_{\mathrm{O}} - y}{x_{\mathrm{O}} - x}\right) + \frac{\pi}{2} \tag{7}$$

and given $(x_{\mathrm{O}}, y_{\mathrm{O}})$ is the location of the center of the orbit and (x, y) is the location of the UA. The resulting periodic motion of a UA following this orbit trajectory will allow for transects to be made across the RFGF in the area sampled during the VORTEX2 operations. The radius of the orbit, and thus the transect distance has been reduced from the typical 5km to 1km, so the UA performs more orbits during

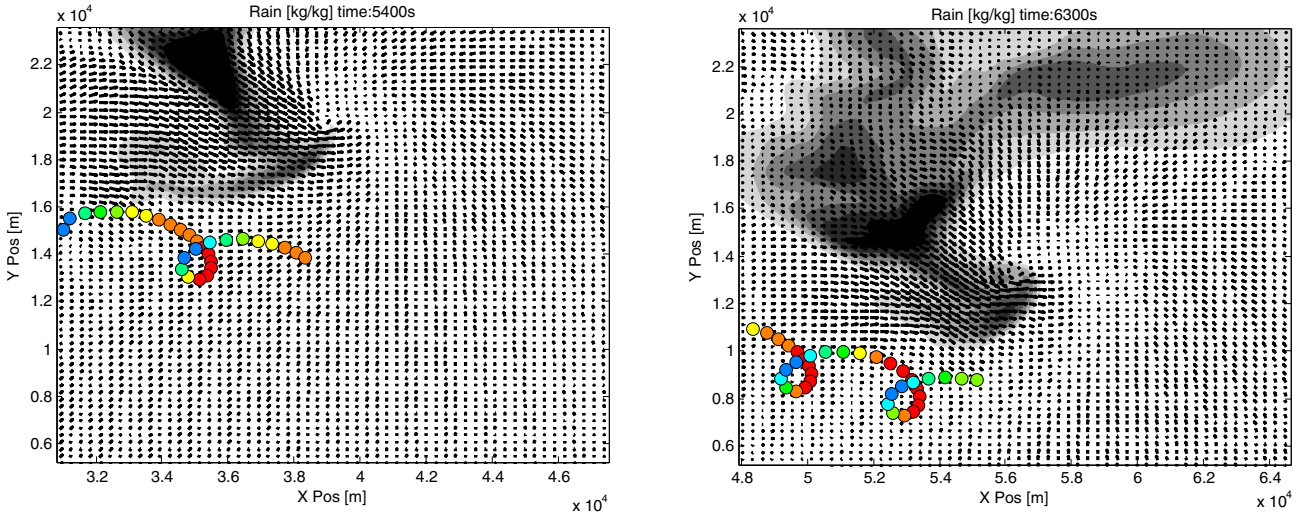

Fig. 5. A time series of the simulated storm and flight path. The flight path has been colored based on the amount of energy in the UA system, with blue being the highest and red being the lowest.

the 20 minutes of simulated storm data. This might affect the quality of the sampled data, but must also be balanced with the required radius for effective dynamic soaring, which is typically much smaller than 1km. An investigation as to the feasibility and value of changing the orbit radius is left to future work.

In order to track the RFGF and the sampling location 5 km south of the hook echo for the full 20 minutes of simulated storm data, it was necessary to move the center of the orbit pattern. This was done through linear interpolation of the desired location for sensing at the start of the simulation and end of the simulation. This movement of the orbit center along with stronger west to east winds produced the spiraling motion of the aircraft flight path, shown in Figure 5. Note that the axes scales remain constant as the axis labels change according to the translation of the storm in the inertial frame. Given the limited timespan of the data, and the ability to easily identify features such as the RFGF and hook echo, the tracking of the desired center location of the orbit was a relatively simple task to perform manually. However, in real-world situations this might not be so easy, especially considering the wind environment will not be as well known as it is in the simulation. The location of the center of the orbit will not only need to move according to the progression of the gust front, as demonstrated by this simulated storm, but the translation of the hook echo must also considered for the aircraft to avoid dangerous regions of the supercell. As was done here, human determination of the location of the hook echo is possible through examination of reflectivity data, that might be sent to the aircraft. However, the winds in the RFGF will not be well defined and an automatic algorithm will probably be needed to keep the orbit center in the optimal location for harvesting energy.

Figure 5 shows the results from one simulated run. The UA was initialized on the orbit path and utilized a PID controller to maintain a radius from the orbit center and the correct altitude. The color of the track is used to indicate the amount of energy at intervals during the simulation found using:

$$e_{TOTAL} = g \cdot h + \frac{1}{2}mv^2 \tag{8}$$

In Figure 5, blue indicates a relatively high energy level, and red a relatively low energy level.

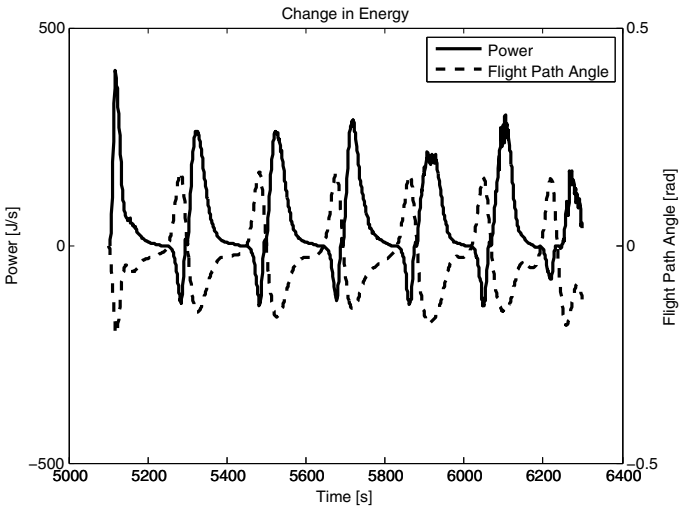

Fig. 6. Change in energy and flight path angle for a simulated flight using 100 m deviation from center point in altitude across the sampling pattern, and an orbit radius of 1 km.

Figure 6 better indicates the amount of energy gained by the system through employing dynamic soaring. Here the change in energy, derived using Equation 3, is shown along with the flight path angle. This indicates the expected increase in energy on the downwind, descending leg, as is typically witnessed in dynamic soaring applications [16].

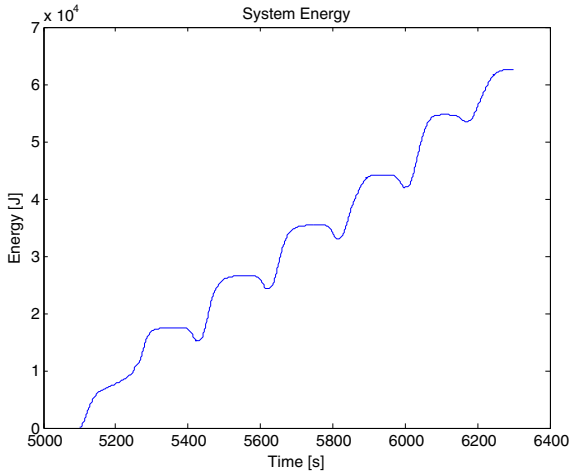

Fig. 7. System energy for a simulated flight using 100 m deviation from center point in altitude across the sampling pattern, and an orbit radius of 1 km.

However, well beyond simply adding some energy to the system, the net result is a significant increase (Figure 7). Further examining the storm structure reveals why this is the case. Unlike typical dynamic soaring applications, that simply require that the strength of the horizontal winds increase with altitude, the gust front contains additional features that enhance the energy extraction process. Figure 3(b) shows two of these features. First, the lower level winds are part of the inflow and arriving from the east, in the opposite direction of the higher level winds encountered in the flight path on the west side of the RFGF. Second, the winds on the west side of the RFGF have a significant positive z component. This increases the amount of energy in the system in a similar fashion to the static soaring approach, and can be seen in Figure 2(b).

V. CONCLUSIONS

The ability to extract energy from supercell thunderstorms was examined, with specific regard to static and dynamic soaring. Regions of the storm were determined to have updrafts significant enough to sustain flight, but poor choices due to their proximity to the hook echo, and relatively small geometry in the horizontal plane. An examination was also performed to determine if a sUAS could employ dynamic soaring techniques to simultaneously sample and gain energy. Simulated flights indicate the promising result that energy can be harvested in this manner, however they also indicate a need for the determination of the optimal orbit to improve the amount of energy obtained from each orbit. Future work will also include an analysis of the effect of the radius of the orbit and changes in altitude across the orbit on the ability to extract energy. Given that the distance to the hook echo is approximately 5 km, increasing the radius too much in the y direction will put the aircraft in dangerous parts of the storm to perform its sampling mission. The pattern geometry might need to be modified to limit the deviation of the aircraft from the x axis of the orbit.

ACKNOWLEDGMENT

This paper is based upon work supported by the National Science Foundation under Award No. AGS-1231096.

REFERENCES

[1] National Oceanic and A. Association, "Vortex2: Verification of the origins of rotation in tornadoes experiment," http://www.nssl.noaa.gov/vortex2/, 2010.

[2] P. M. Markowski, "Hook echoes and rear-flank downdrafts: A review," *Monthly Weather Review*, vol. 130, no. 4, pp. 852–876, 2002.

[3] J. D. Marwitz, "The structure and motion of severe hailstorms. part i: Supercell storms," *Journal of Applied Meteorology*, vol. 11, pp. 166–179, 1971.

[4] J. S. Elston, J. Roadman, M. Stachura, B. Argrow, A. Houston, and E. W. Frew, "The tempest unmanned aircraft system for in situ observations of tornadic supercells: Design and vortex2 flight results," *Journal of Field Robotics*, vol. 28, no. 4, pp. 461–483, July 2011. [Online]. Available: http://onlinelibrary.wiley.com/doi/10.1002/rob.20394/abstract

[5] K. Andersson, I. Kaminer, K. Jones, V. Dobrokhodov, and D.-J. Lee, "Cooperating uavs using thermal lift to extend endurance," in *AIAA Infotech@Aerospace Conference*, Seattle, WA, Apr. 2009.

[6] A. Chakrabarty and J. Langelaan, "Energy-based long-range path planning for soaring-capable unmanned aerial vehicles," *AIAA Journal of Guidance, Control, and Dynamics*, vol. 34, no. 4, pp. 1002–1015, 2011.

[7] G. Sachs, "Minimum shear wind strength required for dynamic soaring of albatrosses," *Ibis*, vol. 147, no. 1, pp. 1–10, 2005.

[8] P. Lissaman, "Wind energy extraction by birds and flight vehicles," *AIAA paper*, vol. 241, 2005.

[9] P. L. Richardson, "How do albatrosses fly around the world without flapping their wings?" *Progress in Oceanography*, vol. 88, no. 1, pp. 46–58, 2011.

[10] J. Langelaan, N. Alley, and J. Neidhoefer, "Wind field estimation for small unmanned aerial vehicles," in *AIAA Guidance, Navigation, and Control Conference*, Toronto, ON, August 2010.

[11] J. Elston and E. W. Frew, "Unmanned aircraft guidance for penetration of pre-tornadic storms," *AIAA Journal of Guidance, Control, and Dynamics*, vol. 33, no. 1, pp. 99–107, January 2010. [Online]. Available: http://arc.aiaa.org/toc/jgcd/33/1

[12] L. Rayleigh, "The soaring of birds," *Nature*, vol. 27, no. 701, pp. 534–535, 1883.

[13] G. Sachs and O. da Costa, "Optimization of dynamic soaring at ridges," in *AIAA Atmospheric Flight Mechanics Conference and Exhibit, Austin, Texas*, 2003, pp. 11–14.

[14] O. Ariff and T. Go, "Waypoint navigation of small-scale uav incorporating dynamic soaring," *Journal of Navigation*, vol. 64, no. 01, pp. 29–44, 2011.

[15] P. L. Richardson, "High-speed dynamic soaring," 2012.

[16] C. Gao and H. H. Liu, "Dynamic soaring surveillance in a gradient wind field," ser. AIAA Guidance, Navigation, and Control and Co-located Conferences. American Institute of Aeronautics and Astronautics, August 2013. [Online]. Available: http://dx.doi.org/10.2514/6.2013-4863

[17] J. J. Bird, J. W. Langelaan, C. Montella, J. Spletzer, and J. Grenestedt, "Closing the loop in dynamic soaring," 2014.

[18] N. Depenbusch and J. Langelaan, "Receding horizon control for atmospheric energy harvesting by small uavs," in *AIAA Guidance, Navigation, and Control Conference*, Toronto, ON, August 2010.

[19] J. Elston, B. Argrow, E. Frew, A. Houston, and J. Straka, "Evaluation of UAS Concepts of Operation for Severe Storm Penetration using Hardware-in-the-Loop Simulations," *AIAA Journal of Aerospace Computing, Information, and Communication*, vol. 8, no. 9, pp. 269–294, September 2011. [Online]. Available: http://arc.aiaa.org/toc/jacic/8/9

[20] A. Bott, "Cloud and precipitation microphysics by jerry m. straka," *Boundary-Layer Meteorology*, vol. 135, pp. 177–178, 2010, 10.1007/s10546-009-9454-7. [Online]. Available: http://dx.doi.org/10.1007/s10546-009-9454-7

[21] J. M. Roadman, J. Elston, B. Argrow, and E. Frew, "Performance of the electric-powered tempest uas in supercell storms," *AIAA Journal of Aircraft*, vol. 49, no. 6, pp. 1821–1830, November 2012. [Online]. Available: https://www.aiaa.org/IframeTwoColumn.aspx?id=6009